ISIJ International, Vol. 38 (1998), No. 8, pp. 834–842

Heat Transfer across Mold Flux Film in Mold during Initial Solidification in Continuous Casting of Steel

Jung Wook CHO, Toshihiko EMI,[1] Hiroyuki SHIBATA[1] and Mikio SUZUKI[1]

Graduate Student, Tohoku University, Katahira, Aoba-ku, Sendai, Miyagi-ken, 980-8577 Japan.
1) Institute for Advanced Materials Processing, Tohoku University, Katahira, Aoba-ku, Sendai, Miyagi-ken, 980-8577 Japan.

(Received on January 30, 1998; accepted in final form on April 2, 1998)

Analysis of heat transfer near the meniscus in mold for continuous casting of steel has been carried out by taking into account conductive and radiative thermal resistances of infiltrated mold flux film and thermal resistance at the copper mold/solidifying mold flux film interface. Mold fluxes in commercial use for casting low and medium carbon steel are selected for this study. Thermal conductivities, absorption coefficients and interfacial thermal resistances of these fluxes have been determined in our previous work by laser flash method, high temperature cell FTIR test and contacting thermal resistance test, respectively. Calculation with these data shows that the heat transfer is strongly influenced by the interfacial thermal resistance. Slow cooling required for casting surface crack sensitive medium carbon peritectic steel slabs can be achieved by making the interfacial thermal resistance high, which is attainable by use of basic mold fluxes with high rate of crystallization. A flux film thicker than 0.25 mm for the low carbon steel or 0.4 mm for the medium carbon steel is also found to be a requisite to prevent the occurrence of longitudinal surface cracks. Reasonably high interfacial thermal resistance and a proper flux film thickness are essential to reduce the surface defects and to increase the speed of continuous casting of these steel slabs.

KEY WORDS: heat transfer; mold flux; conductivity; absorption coefficient; interfacial thermal resistance; continuous casting.

1. Introduction

Occurrence of surface defects on continuously cast steel slabs is strongly influenced by the heat transfer during initial solidification of the slabs in mold. Excessively large heat flux, for example, causes longitudinal surface cracks on the slabs,[1] and hence control of the heat flux in the mold based on a reliable heat analysis is an important issue to produce defect free slabs.

Many efforts have been concentrated on reducing the heat flux by increasing thermal resistance provided by mold flux film which infiltrates between the mold and solidifying steel shell. The mold flux film for casting low carbon or medium carbon steel slab is shown, by the observations[1–3] on the mold flux film beneath the meniscus, to consist of two vertical parallel layers, melt and crystalline solid. The two layers provide the film with thermal resistances to the conductive and radiative heat transfers in the mold.[4] In addition, experimental studies show that another thermal resistance caused by the air gap at mold/mold flux film interface plays an important role in the heat transfer in the mold.[4–8] Thus, consideration on the thermal resistances arising from the molten layer, crystalline layer and the air gap is essential to carry out the heat transfer analysis in the mold.

Early studies[9–11] on the heat transfer ignored, however, the phase separation of the mold flux film. Instead, these studies assumed an average thermal conductivity for whole flux film thickness. This could result in some error in calculating the heat flux because a thickness ratio of the molten layer to crystalline layer each having different thermophysical properties influences the heat transfer in the mold. Also, the dimension of the air gap at the copper mold/solidifying flux film interface was evaluated to be equivalent to the shrinkage of solidifying steel shell by assuming a constant mold flux film thickness which was calculated from observed consumption rate of the mold flux.[10,11] Analysis on such evaluation and assumption gives excessively large interfacial thermal resistance[11] which makes temperature so high at the air gap/mold flux film interface that the film is melted all through the thickness.

Recently, the authors have determined both the conductive and radiative thermal conductivities of mold fluxes with a laser flash[12] and a high temperature FTIR methods, respectively.[13] Also, they have determined the interfacial thermal resistance as a function of the crystalline layer thickness of mold flux film.[5]

The aim of this study is to carry out a reliable calculation of the heat transfer near the meniscus portion in continuous casting mold by utilizing these own experimental data, making it possible to control the heat transfer and minimize the surface cracks.

Table 1. Chemical composition (in mass%) and physical properties of mold fluxes used.

Mold flux	LC2	MC2
Steel grade applied	low carbon	medium carbon
SiO_2	35.0	31.8
CaO	33.8	44.8
Al_2O_3	6.4	3.7
Fe_2O_3	0.7	0.4
Na_2O	11.2	7.3
MgO	2.3	1.9
MnO	0.1	0.1
TiO_2	0.1	0.1
K_2O	0.5	0.3
Li_2O	4.6	3.9
F	8.4	9.9
CaO/SiO_2	0.96	1.41
Viscosity (Pa·s at 1573K)	0.09	0.05
Crystallizing temperature(K)	1316	1436
thermal conductivity (W/m.K)	1.73 (cry.)[12]	1.83 (cry.)[12]
	1.33 (melt)[12]	

2. Method of Calculation and Preliminary Results

2.1. Properties of Mold Fluxes Investigated

Among the commercial mold fluxes investigated in previous studies,[5,13] two mold fluxes listed in **Table 1**, one for high speed casting of low carbon steel (LC2) and the other for medium carbon steel (MC2), were selected for calculation. The MC2 flux is featured by higher basicity and higher crystallizing temperature.

2.2. Thermal Resistance at Mold Flux Film/Mold Interface

Thermal resistance for the heat transfer from solidifying steel shell to mold consists of conductive, radiative and interfacial components as shown in **Fig. 1**. Among these components, interfacial thermal resistance has been observed[5] [R_{INT}(obs.)] as shown in **Fig. 2** under similar circumstances to those in actual casting mold as a function of the crystalline layer thickness, d_{CRY}, which is the difference between the total flux film thickness, d_{FLUX}, and the melt layer thickness, d_{MELT}, in the mold flux film, by

$$R_{INT}(\text{obs.})(10^{-4}\,\text{m}^2\,\text{K/W}, \text{ for LC2}) = 2.94 d_{CRY}(\text{mm}) + 3.52, \quad \text{for } 0.3\,\text{mm} \leqq d_{CRY} \leqq 1.0\,\text{mm} \quad \ldots\ldots(1)$$

$$R_{INT}(\text{obs.})(10^{-4}\,\text{m}^2\,\text{K/W}, \text{ for MC2}) = 16.4 d_{CRY}(\text{mm}), \quad \text{for } 0.4\,\text{mm} \leqq d_{CRY} \leqq 0.9\,\text{mm} \quad \ldots\ldots(2)$$

The d_{CRY} of MC2 is larger than that of LC2 due to higher basicity and higher crystallizing temperature. Also, Eqs. (1) and (2) show that R_{INT}(obs.) is higher for MC2 than for LC2 even at the same d_{CRY}. One of the reasons for this difference can be attributed to the fact that observed crystallization rate[14] of MC2 is faster than that of LC2.

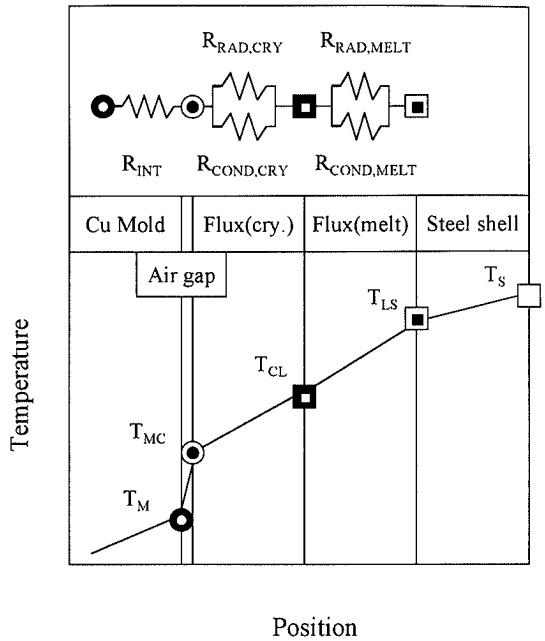

Fig. 1. Schematic of temperature distribution and resistances to heat transfer across mold flux film consisting of crystalline and molten layers.

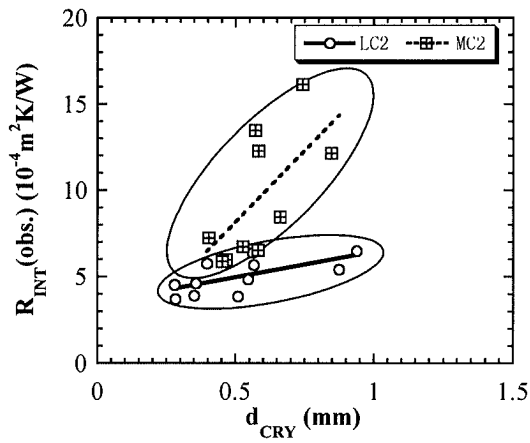

Fig. 2. Change of observed interfacial thermal resistance with thickness of crystalline layer of mold flux film.

The R_{INT}(obs.) after Eqs. (1) and (2) agrees well with the previous observations[1,7] that MC mold fluxes give smaller heat flux than LC mold fluxes.

2.3. Heat Flux

The total heat flux, q_{TOT}, through mold flux film near the meniscus portion in the mold is calculated as a function of d_{FLUX} according to the flowchart shown in **Fig. 3**. Following assumptions are used in the calculation:

- mold flux film consists of crystalline and molten layers in parallel and in contact,
- heat flows one dimensionally from solidifying steel shell through the molten and crystallized layers of infiltrated mold flux film to copper mold in a steady state,
- there is no interaction between the radiation and conduction, and
- mold flux behaves like gray gas[15] for the radiative heat transfer.

Thus, q_{TOT} for the molten layer can be expressed as

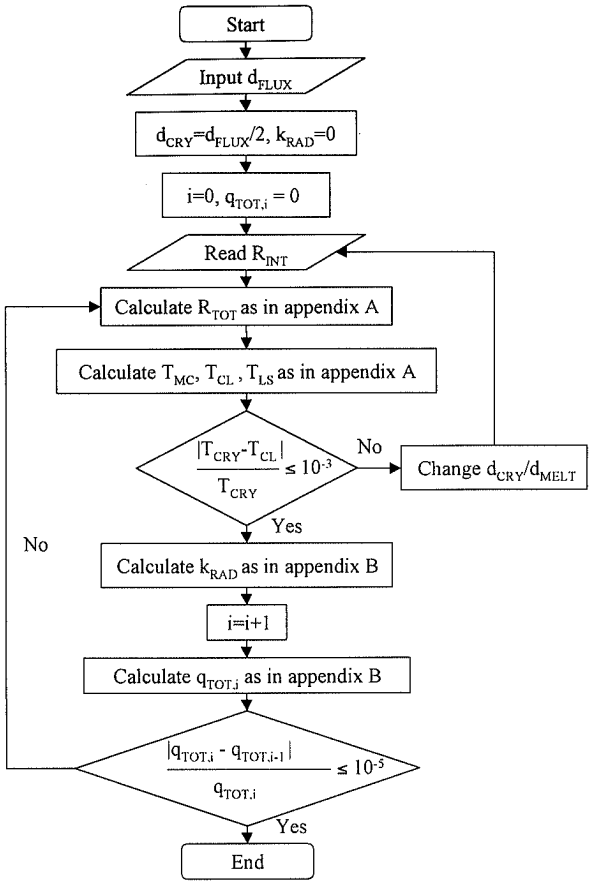

Fig. 3. Flowchart for calculating heat flux in mold for experimental range of mold flux film thickness in Eqs. (1) and (2).

Table 2. Conditions and physical properties for mold heat flux calculation.

casting speed (m/min)	2.0 (LC2) 1.6 (MC2)
position	30mm below the meniscus
solidifying steel shell thickness (mm)	15 $t^{1/2}$ [16] (t:min)
interfacial thermal resistance (m^2KW^{-1})	Eqs. 1 and 2
thermal conductivity (W/m.K)	31.1 (steel shell) [17] 383 (copper mold) [17]
emissivity	0.8 (steel shell) [18] 0.4 (copper mold) [18] 0.7 (crystalline flux) [18]
Mold surface temperature (K)	593
solidus temperature of steel (K)	1780 (low carbon steel) 1749 (medium carbon steel
crystallizng temperature of mold flux (K)	1316 (LC2) 1436 (MC2)

$$q_{TOT}=k_{EFF,MELT}(T_{LS}-T_{CL})/d_{MELT} \quad \cdots\cdots (3)$$

which should be equal to

$$q_{TOT}=k_{EFF,CRY}(T_{CL}-T_{MC})/d_{CRY} \quad \cdots\cdots (4)$$

for the crystalline layer as shown in Fig. 1.
Here,

$$k_{EFF,MELT}=k_{COND,MELT}+k_{RAD,MELT} \quad \cdots\cdots (5)$$

$$k_{EFF,CRY}=k_{COND,CRY}+k_{RAD,CRY} \quad \cdots\cdots (6)$$

In Eqs. (3)–(6), k_{COND} or k_{RAD} is conductive or radiative

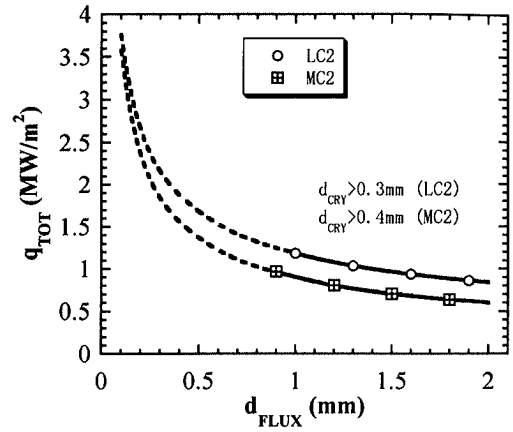

Fig. 4. Calculated heat flux near the meniscus in mold.

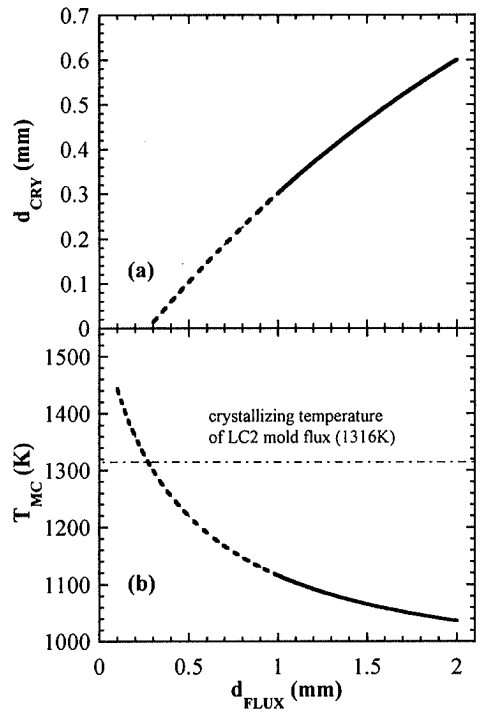

Fig. 5. Change of crystalline layer thickness and temperature at the interface of copper mold/crystalline layer of LC2 mold flux film.

thermal conductivity, and $(T_{CL}-T_{MC})$ or $(T_{LS}-T_{CL})$ is the difference in temperatures on both sides of crystalline or molten layer as shown in Fig. 1. Details of derivation of k_{RAD} shown in Fig. 3 is given in Appendix B, and conditions and physical properties[16–18] used for the calculation are given in **Table 2**.

Results of the calculation are shown in **Fig. 4**. R_{INT}(obs.)'s are available only in the range of d_{CRY} thicker than 0.4 mm for MC2 or 0.3 mm for LC2 (see Fig. 2) each of which is calculated from corresponding d_{FLUX} of 0.9 mm for MC2 or 1.0 mm for LC2.

2.4. Threshold Interfacial Thermal Resistance

As the calculation of the heat flux below the above critical flux film thicknesses becomes speculative, relation between d_{CRY} and d_{FLUX} obtained from the calculation shown in Fig. 3 is plotted as a solid line in **Fig. 5(a)**. If Eq. (1) for R_{INT}(obs.) of LC2 is extrapolated to the range

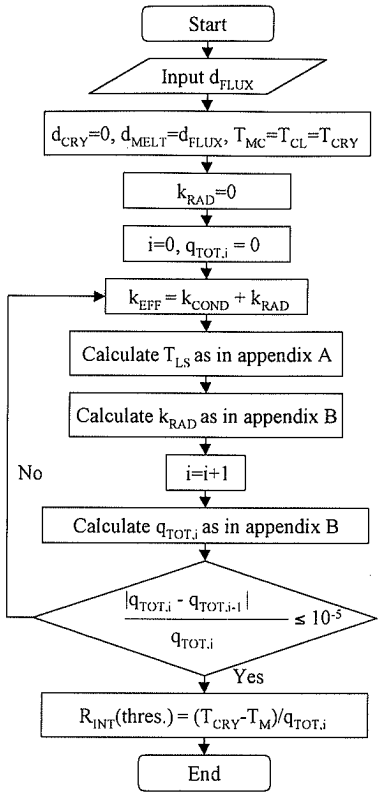

Fig. 6. Flowchart for calculating threshold interfacial thermal resistance.

of d_{CRY} of less than 0.3 mm, the crystalline layer disappears at d_{FLUX} of 0.3 mm which is the intersect of the broken line with the horizontal axis in Fig. 5(a). As shown in **Fig. 5(b)**, this is caused by the fact that calculated temperature at the interface between the air gap and crystalline layer (T_{MC}) exceeds the melting point of LC2.

Previous observations[2,5,8] have shown, however, that R_{INT} arises from solid/solid contact between the solidifying (in this case, crystallizing) mold flux film and copper mold. Thus, R_{INT} is meaningful only when d_{CRY} is positive, and hence one can define a threshold value, R_{INT}(thres.), as R_{INT} at d_{CRY} is zero.

The R_{INT}(thres.) is calculated according to the flow chart shown in **Fig. 6** under the condition that crystalline layer is about to disappear. Assumptions and physical properties used in this calculation are all the same as those listed in Table 2. Calculated R_{INT}(thres.) for both fluxes are shown in **Fig. 7**. For LC2, R_{INT} obtained by the linear extrapolation of Eq. (1) (dotted line in Fig. 7) exceeds R_{INT}(thres.) in the range less than 0.3 mm of d_{FLUX}, which is the same range where crystalline layer disappears in Fig. 5(a). This inconsistency results from inadequacy of the linear extrapolation in obtaining R_{INT} at $d_{CRY}<0.3$ mm.

To resolve the inconsistency, R_{INT}(obs.) is normalized by R_{INT}(thres.) and plotted against d_{FLUX} in **Fig. 8**. Here, extrapolation of R_{INT}(obs.)/R_{INT}(thres.) to the range where $d_{FLUX}<0.9$–1.0 mm converges reasonably between 0.4 to 0.8 at $d_{FLUX}=0$. This ratio is used to calculate q_{TOT} according to the flow chart shown in **Fig. 9** where the extrapolation of the ratio in Fig. 8 replaces that of R_{INT} in Fig. 2 in the range of $d_{FLUX}<0.9$–1.0 mm. In this

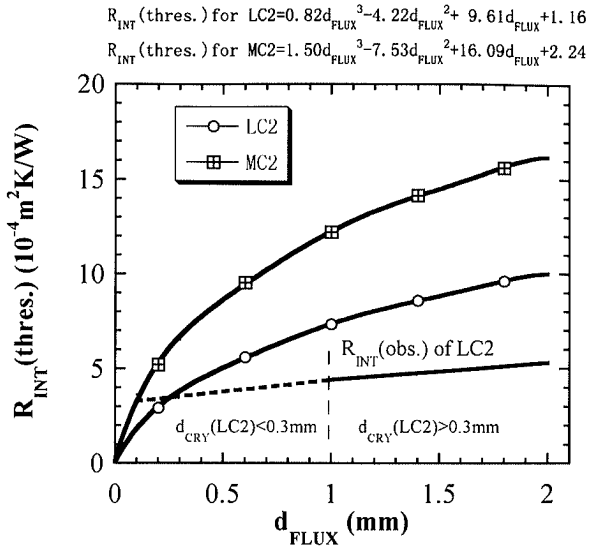

Fig. 7. Change of threshold interfacial thermal resistance with total mold flux film thickness.

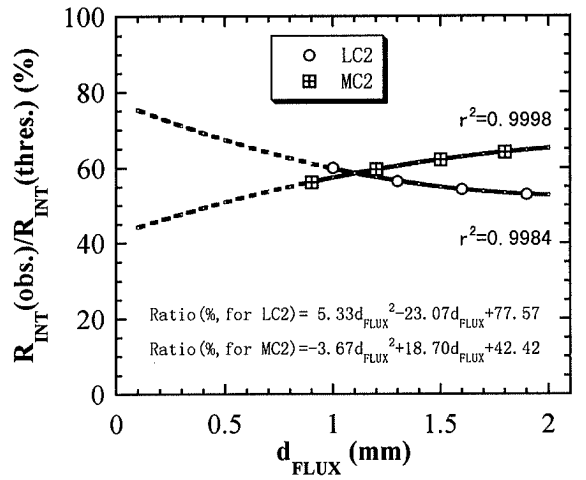

Fig. 8. Change of ratio of observed to threshold interfacial thermal resistances with total flux film thickness.

way, q_{TOT} across the mold flux film can be calculated for the whole range of d_{FLUX} to be shown in Sec. 3.1.

3. Results and Discussion

3.1. Total Heat Flux

Calculated total heat flux, q_{TOT}, as shown in **Fig. 10**, decreases exponentially with increasing flux film thickness for both LC2 and MC2. The q_{TOT} for LC2 is always higher than that for MC2 at the same film thickness. Critical heat fluxes, beyond which longitudinal surface cracks on slabs of similar grades of steel were reported to occur with similar mold fluxes, are also shown in Fig. 10. According to this figure, one must control the flux film to be thicker than 0.25 mm for LC2 or 0.4 mm for MC2 to avoid the occurrence of the longitudinal cracks.

Mold flux film thickness near the meniscus was measured by Kanazawa *et al.*[1] at different casting speed, V_C, and was given by

$$d_{FLUX}=0.9464V_C^{-0.4895} \quad \text{.....(7)}$$

Chemical composition, crystallizing temperature and viscosity of the mold fluxes used in their study are sim-

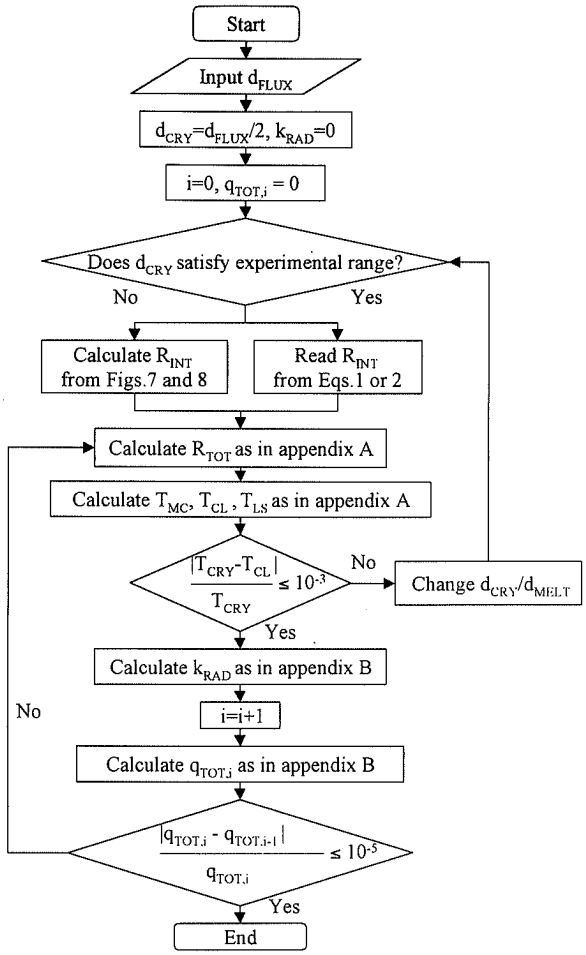

Fig. 9. Flowchart for calculating heat flux in mold for whole range of flux film thickness.

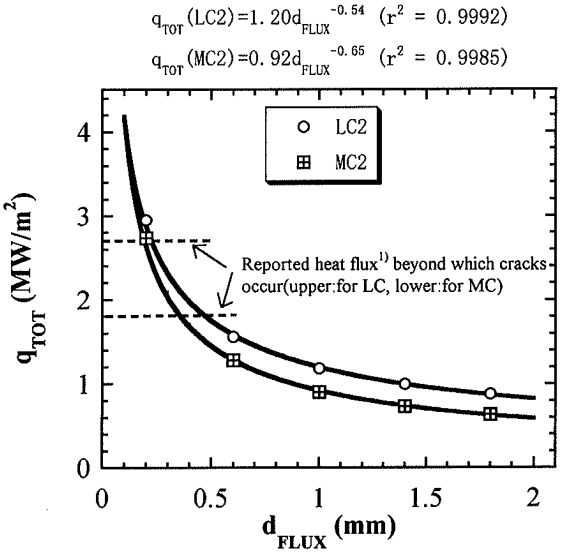

Fig. 10. Heat flux in mold as a function of total mold flux film thickness.

ilar to those of the present study, and hence Eq. (7) may approximate d_{FLUX} to be 0.67 mm for LC2 at V_C of 2.0 m/min and 0.75 mm for MC2 at V_C of 1.6 m/min (ref. Table 2 for the V_C's). These flux film thicknesses are larger than the critical ones below which longitudinal surface cracks are reported to occur as shown in Fig. 10.

At these d_{FLUX}'s, 0.67 mm for LC2 and 0.75 mm for

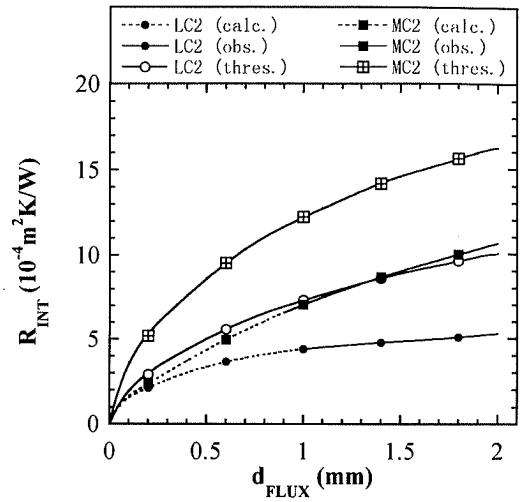

Fig. 11. Comparison of threshold interfacial thermal resistance with calculated or observed ones.

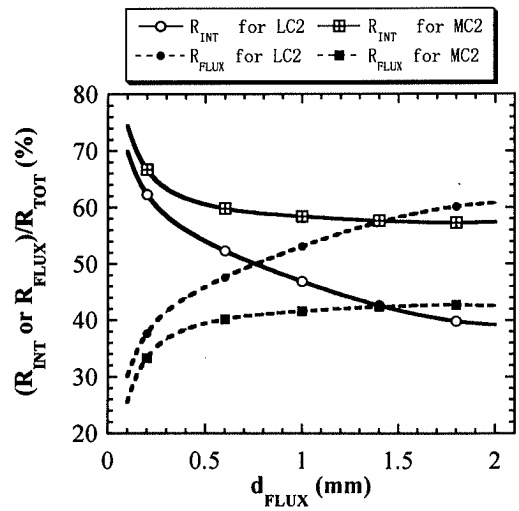

Fig. 12. Change with total flux film thickness of thermal resistance ratio of interfacial (R_{INT}) or flux film (R_{FLUX}) to total (R_{TOT}).

MC2, q_{TOT} for MC2 becomes *ca.* 25% less than that of LC2 as shown in Fig. 10. This agrees well with plant observations that heat flux near the meniscus in mold is lower in casting medium carbon steels than in casting low carbon steels. The reason for the slow cooling with MC2 is due to the fact that R_{INT} of MC2 is always larger than that of LC2 as shown in **Fig. 11**. For example, at 0.67 mm for LC2 and 0.75 mm for MC2, R_{INT} of MC2 (5.82×10^{-4} m^{2}K/W) is *ca.* 50% larger than that of LC2 (3.84×10^{-4} m^{2}K/W). In addition, the ratio of R_{INT} to R_{TOT} ($=R_{INT}+R_{FLUX}$) becomes *ca.* 50% for LC2 and 60% for MC2 at the above values of d_{FLUX} for LC2 and MC2 as shown in **Fig. 12**. Thus, these calculations show that R_{INT} plays most important role in the heat transfer in mold, *i.e.*, higher interfacial thermal resistance resulting from higher crystallizing temperature is the main reason for the slower cooling (lower q_{TOT}) with MC2 mold flux.

The relation between R_{INT} and d_{CRY} is calculated and shown in **Fig. 13**, which is similar to that given in Fig. 11. The decrease of R_{INT} with decreasing d_{CRY} for MC2 is almost the same as that expressed by Eq. (2) where

the decrease of R_{INT} for LC2 in the same range of d_{FLUX} is much more than that by Eq. (1). Extrapolation of the regression curves in Fig. 13 for the two fluxes tends to converge to origin. This is believed reasonable in view of the fact that the crystallizing of the mold flux is the cause of interfacial thermal resistance.[5] Conversely, when the mold flux does not yield crystalline layer ($d_{CRY}=0$), no interfacial thermal resistance arises resulting in excessive cooling of solidifying steel shell.

3.2. Contribution of Radiative Heat Transfer to Total Heat Transfer

Fraction of radiative heat transfer in total heat transfer across the mold flux film during initial solidification in continuous casting mold has been a controversial issue in the past investigations, varying from 20 to 50%[4,7,8,13,19] for the molten layer of mold flux film as listed in **Table 3**. The fraction is, therefore, reevaluated on the basis of the present study. The radiative heat flux, q_{RAD}, across molten layer only of flux film increases with increasing d_{FLUX} and hence with increasing d_{MELT} as shown in **Figs. 14(a)** and **14(b)**. This is a consequence of the increase of temperature, T_{LS}, at the molten layer/steel shell interface with increasing d_{FLUX} and d_{MELT} as indicated by Eqs. (A-7) and (A-8) in the Appendix.

The ratio of q_{RAD} to q_{TOT} for the molten layer of flux film reaches from 35 to 50% when d_{MELT} varies from 0.6 to 1.0 mm for d_{FLUX} varing from 1.0 to 1.5 mm, which is about the same range of flux film thickness as listed in Table 3. This ratio agrees well with our previous calculation (46% for LC2 and 37% for MC2)[13] but somewhat larger than those estimated by others.[4,7,8,19] Such difference mainly comes from higher surface temperatures, T_{CL} and T_{LS}, in our case than in others case as shown in Table 3.

For crystalline layer of flux film, the ratio of radiative heat flux to total reaches only 4% when d_{CRY} varies from 0.3 to 0.6 mm due to much larger extinction coefficient and lower surface temperature of the crystalline layer.

3.3. Effective Thermal Conductivity

Radiative thermal conductivity, k_{RAD}, can be calcu-

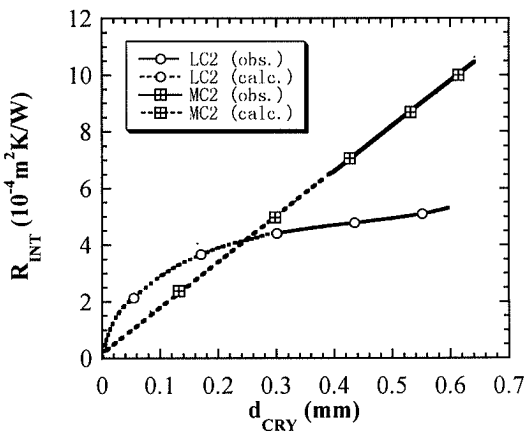

Fig. 13. Relationship between interfacial thermal resistance and crystalline layer thickness.

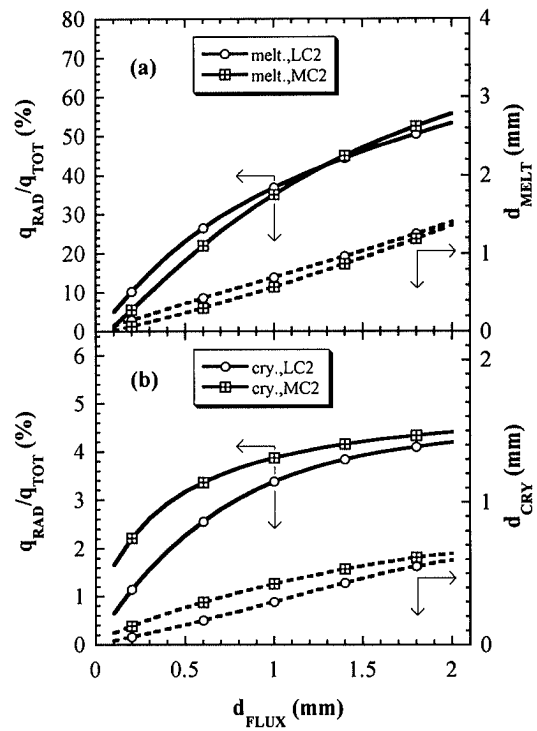

Fig. 14. Change of ratio of radiative heat flux to total heat flux with thicknesses of crystalline layer, molten layer and total film.

Table 3. Reported values on the contribution of radiative heat transfer.

Researcher	Surroundings	Temperature (K)	Basicity (CaO/SiO_2)	Flux thickness (mm)	q_{RAD}/q_{TOT} (%)	Method
Yamauchi[8]	SUS/l*1/AlN	923-1073/1373	1.1*4	0.58*5	20 (melt)	Est.
Ohmiya[4]	Cu/(l+c)*2/Fe,Mo	323-423/773-1773	1	1-3	26-50 (melt+cry.)	Est.
Watanabe[7]	Cu/(g+c)*3/l	573/1673	1.47	0.7*5	36 (melt) 13 (cry.)	Est.
Kawamoto[19]	Cu/ (l+c)/Mo	573/1373	1.1	1.2	27 (melt) 6 (cry.)	Est.
Cho[13]	Cu/(l+c)/Fe	593/1723	0.96 (LC2) 1.41 (MC2)	1.5	46 (LC2, melt) 37 (MC2, melt) 4 (LC2 & MC2, cry.)	Calc.

*1: molten flux, *2: flux with coexistent melt and crystalline solid, *3: partially crystallized glassy flux,*4: synthetic flux with melting point of 923K, *5: molten layer thickness

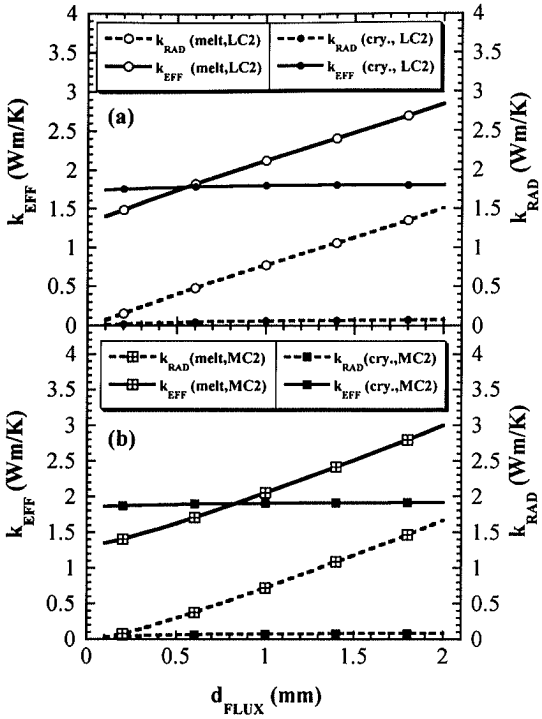

Fig. 15. Change of effective and radiative thermal conductivities of crystalline and molten layers with total flux film thickness.

lated from q_{RAD} as

$$k_{RAD}(\text{cry.}) = q_{RAD} d_{CRY} / (T_{CL} - T_{MC}) \quad \text{.....(8)}$$

and

$$k_{RAD}(\text{melt}) = q_{RAD} d_{MELT} / (T_{LS} - T_{CL}) \quad \text{.....(9)}$$

It has been shown in our previous study[6] that k_{COND} remains constant with temperature for both crystalline and molten layers. Accordingly, the change of k_{EFF} ($=k_{COND}+k_{RAD}$) is due to the change of k_{RAD}. The k_{EFF}, and hence k_{RAD}, for molten layer linearly increases whereas that for crystalline layer remains almost unchanged with d_{FLUX} as shown in **Figs. 15(a)** and **15(b)**. It is to be noted here that k_{EFF} for crystalline layer is about the same as that of molten layer when d_{FLUX} is 0.67 mm for LC2 or 0.75 mm for MC2, which is about the same flux film thickness in actual mold as calculated by Eq. (7). There have been several attempts made to explain the mechanism of slow cooling attainable in slab casting mold by the application of mold fluxes with $CaO/SiO_2 > 1$ in terms of the reduction of radiative heat flux caused by the scattering of radiation at the grain boundaries of crystals in the crystalline layer of flux films.[1,9,20,21] However, as shown in Figs. 14 and 15, the reason for the slow cooling is not due to the reduction of radiative heat transfer but due mainly to the increase of R_{INT} with the thickness of crystalline layer as a consequence of increased crystallizing temperature with basicity.[13]

3.4. Effect of Mold Temperature, Casting Speed and Mold Flux Properties on Heat Flux

The effect of mold surface temperature, T_M, on q_{TOT} is examined by lowering T_M from 593 to 553 K. As shown

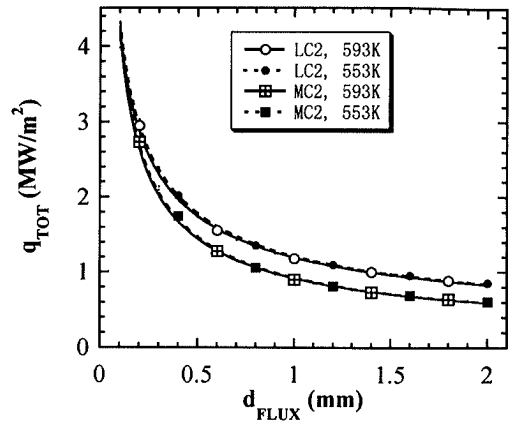

Fig. 16. Effect of mold surface temperature on heat flux near meniscus in mold.

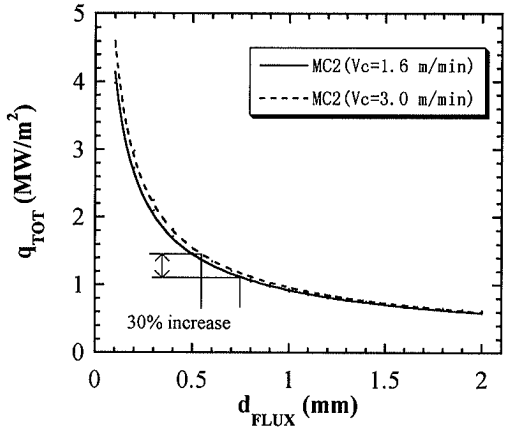

Fig. 17. Effect of casting speed on heat flux near meniscus in mold.

in **Fig. 16**, the difference in q_{TOT} by lowering T_M is only 2.2% for LC2 and 1.6% for MC2 when d_{FLUX} is 0.67 mm for LC2 and 0.75 mm for MC2. Thus, the influence on q_{TOT} of the difference in T_M between this calculation (593 K) and real operation where T_M may vary from 573 to 623 K[22] can be ignored.

The effect of casting speed, V_C, on q_{TOT} is calculated and shown in **Fig. 17**. Change of V_C from 1.6 to 3 m/min results in *ca.* 5% of increase in q_{TOT} for MC2 at a d_{FLUX} of 0.75 mm. However, increased V_C also results in decreased d_{FLUX}. At V_C of 3 m/min, Eq. (7) predicts that d_{FLUX} decreases to 0.55 mm. Including the above thinning of d_{FLUX}, the increase of q_{TOT} with the increase of V_C from 1.6 to 3 m/min becomes a high 30%.

With respect to the properties of mold fluxes, absorption coefficients are largely the same for various mold fluxes.[13] Even when the absorption coefficients are made 10 times larger, the decrease in q_{TOT} at d_{FLUX} of 0.67 mm for LC2 and 0.75 mm for MC2 remains to be less than 2% as shown in **Fig. 18**. Thus, attempt to reduce q_{TOT} by applying a mold flux with higher absorption coefficient is hardly effective.

If it is assumed that the crystallizing temperature varies ± 50 K for MC2, resulting difference in q_{TOT} becomes *ca.* ± 8% at a d_{FLUX} of 0.75 mm as shown in **Fig. 19**. Therefore, if the flux consumption rate is kept constant, slower cooling can be effectively achieved by increasing

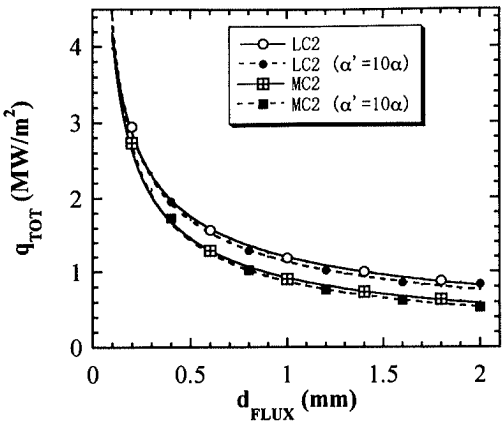

Fig. 18. Effect of increasing absorption coefficient on heat flux near meniscus in mold.

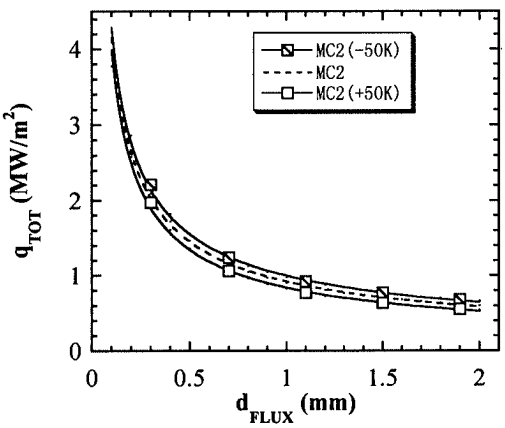

Fig. 19. Effect of change of crystallizing temperature on heat flux near meniscus in mold.

crystallizing temperature either by raising basicity of or by adding proper flux component to the mold flux.

4. Conclusion

Heat flux from solidifying steel shell across infiltrated mold flux film to copper mold at the initial stage of solidification near the meniscus in continuous casting mold has been determined by using observed radiative, conductive and interfacial thermal resistances of mold flux films. The calculated results are summarized as follows:

(1) The heat flux calculated for the mold fluxes for low carbon steel (LC2) and medium carbon steel (MC2) decreases exponentially with increasing flux film thickness, indicating lower values for MC2 than for LC2 since MC2 has higher interfacial thermal resistance.

(2) Comparison with reported critical heat flux for the occurrence of longitudinal cracks on cast slab surface indicates that a flux film thicker than 0.25 mm for LC2 or 0.4 mm for MC2 is required to prevent the surface cracks.

(3) Ratio of thermal resistance at the flux film/mold interface (R_{INT}) to total thermal resistance from the solidifying steel shell across mold flux film to the mold is *ca.* 50% for LC2 and 60% for MC2 at the flux film thickness of 0.67 mm for LC2 and 0.75 mm for MC2, where the film thicknesses are calculated by an equation based on a plant observation of flux film thickness in actual mold. These ratios show that interfacial thermal resistance plays most important role in the heat transfer in mold.

(4) When mold flux film has a thickness ranging from 1.0 to 1.5 mm, the thickness of molten layer of the film varies from 0.6 to 1.0 mm and crystalline layer from 0.3 to 0.6 mm. In this case, the ratio of radiative heat flux to total heat flux for the molten layer increases from 35 to 50%, while the same ratio reaches only about 4% for the crystalline layer due to larger extinction coefficient and lower surface temperature of the latter.

(5) The effective thermal conductivity for the crystalline layer is about the same as that of molten layer at a flux film thickness of 0.67 mm for LC2 and 0.75 mm for MC2. This shows that the increase of R_{INT}, not the reduction of radiative heat flux, is responsible for the slow cooling at the initial stage of solidification in mold when basic mold flux high in crystallizing temperature is applied.

(6) The effects of variation in mold surface temperature and absorption coefficient of mold flux film on total heat flux are found minor. In contrast, increasing casting speed and decreasing crystallizing temperature of mold flux result in considerable increase in total heat flux.

Acknowledgments

The authors would like to thank Mr. Hidenori Sakai of Kokan Mining Co. for his help with DTA analysis. Also, we would like to thank Shinagawa Refractories Co., Sakai Chemical Industry Co. and Nippon Steel Co. for supplying the mold fluxes investigated.

Nomenclature

c_0: propagation speed of electromagnetic radiation in vacuum (2.9979×10^8 m/s)
d: thickness of each layer in mold flux (m)
e: emissive power (W/m^2)
h: Planck's constant (6.6238×10^{-34} J·s)
k: thermal conductivity (W/m·K)
k_0: Boltzmann constant (1.3803×10^{-23} J/K)
L_C: mold flux for casting low carbon steel
M_C: mold flux for casting crack sensitive medium carbon peritectic steel
n: refractive index
q: heat flux (W/m^2)
q_{TOT}: sum of the heat flux of radiation and conduction (W/m^2)
R: thermal resistance (m^2·K/W)
R_{TOT}: sum of the thermal resistance of air gap and mold flux film (m^2·K/W)
r: correlation coefficient in least square regression analysis
T: temperature (K)
T_{CRY}: crystallizing temperature of mold flux (K)
α_M: mean absorption coefficient (m^{-1})
α_P: apparent mean absorption coefficient (m^{-1})
ε: emissivity
λ: wavelength (m)
σ: Stephan–Boltzmann constant (5.67×10^{-8} W/m^2 K^4)

Subscripts

- b: blackbody
- CL: interface of crystalline mold flux film/molten layer of mold flux film
- COND: conduction
- CRY: crystalline layer of mold flux film
- FLUX: mold flux film
- INT: interface between copper mold and mold flux film
- MELT: molten layer of mold flux
- LS: interface of molten layer of mold flux/steel shell
- M: copper mold surface
- MC: interface of copper mold/ crystalline layer of mold flux film
- MOLD: copper mold
- RAD: radiation
- S: solidus line
- SHELL: solidifying steel shell
- λ: wavelength

REFERENCES

1) T. Kanazawa, S. Hiraki, M. Kawamoto, K. Nakai, K. Hanazaki and T. Murakami: *Tetsu-to-Hagané*, **83** (1997), No. 11, 701.
2) J. Fukuta, T. Kondo, K. Tsutsumi and M. Okumura: Initial Stage of Solidification of Steels, ISIJ, Tokyo, (1994), 68.
3) K. Watanabe: NKK Corp., Japan, private communications, (1997).
4) S. Ohmiya, K.-H. Tacke and K. Schwerdtfeger: *Ironmaking Steelmaking*, **10** (1983), No. 1, 24.
5) J. W. Cho, H. Shibata, T. Emi and M. Suzuki: *ISIJ Int.*, **38** (1998), No. 5, 440.
6) H. Shibata, K. Kondo, M. Suzuki and T. Emi: *ISIJ Int.*, **36** (1996), Supplement, S179.
7) K. Watanabe, M. Suzuki, K. Murakami, H. Kondo, A. Miyamoto and T. Shiomi: *Tetsu-to-Hagané*, **83** (1997), No. 2, 115.
8) A. Yamauchi, K. Sorimachi, T. Sakuraya and T. Fujii: *Tetsu-to-Hagané*, **79** (1993), No. 2, 167.
9) S. Hiraki, K. Nakajima, T. Murakami and T. Kanazawa: Steelmaking Conf. Proc., ISS, (1994), 397.
10) H. Nakato and I. Muchi: *Tetsu-to-Hagané*, **66** (1980), No. 1, 33.
11) L. K. Chiang: PTD Conf. Proc., ISS, **13** (1995), 293.
12) H. Shibata, J. W. Cho, T. Emi and M. Suzuki: Proc. of the 5th Int. Conf. on Molten Slags, Fluxes and Salts, ISS, Sydney, (1997), 771.
13) J. W. Cho, H. Shibata, T. Emi and M. Suzuki: *ISIJ Int.*, **38** (1998), No. 3, 268.
14) J. W. Cho, H. Shibata, M. Suzuki and T. Emi: *Sozaiken Iho* (*Bull. Inst. Adv. Mater. Process., Tohoku Univ.*, in Japanese), **53** (1997), 47.
15) R. Siegel and J. R. Howell: Thermal Radiation Heat Transfer, 3rd Ed., McGraw Hill, New York, (1992), Ch. 15.
16) T. Mizoguchi, S. Ogibayashi and T. Kajitani: *Tetsu-to-Hagané*, **81** (1995), No. 10, 971.
17) Thermophysical Properties Handbook, ed. by K. Kobayashi, Youkendou, Tokyo, (1990), 23.
18) Y. Shiraishi: Handbook of Physico-chemical Properties at High Temperatures, ISIJ, Tokyo, (1988), Ch. 10.
19) M. Kawamoto, Y. Tsukaguchi, N. Nishida, T. Kanazawa and S. Hiraki: *ISIJ Int.*, **37** (1997), No. 2, 134.
20) M. Susa, K. Nagata and K. C. Mills: *Ironmaking Steelmaking*, **20** (1993), No. 5, 372.
21) M. Susa, K. C. Mills, M. J. Richardson, R. Taylor and D. Stewart: *Ironmaking Steelmaking*, **21** (1994), No. 4, 279.
22) B. Thomas: Steelmaking Conf. Proc., ISS, **74** (1991), 105.

Appendix A. Calculation of Interface Temperatures

Total thermal resistance, R_{TOT}, can be given as the sum of thermal resistances between copper mold and molten steel.

$$R_{TOT} = R_{INT} + R_{CRY} + R_{MELT} + R_{SHELL} = R_{INT} + d_{CRY}/k_{EFF(CRY)} + d_{MELT}/k_{EFF(MELT)} + d_{SHELL}/k_{COND(SHELL)} \quad \text{.....(A-1)}$$

Interface temperatures in Fig. 1 can then be calculated as

$$T_{MC} = T_M + (T_S - T_M)R_{INT}/R_{TOT} \quad \text{.....(A-2)}$$

$$T_{CL} = T_{MC} + (T_S - T_M)R_{CRY}/R_{TOT} \quad \text{.....(A-3)}$$

$$T_{LS} = T_{CL} + (T_S - T_M)R_{MELT}/R_{TOT} \quad \text{.....(A-4)}$$

In calculating threshold interfacial thermal resistance as shown in Fig. 6, T_{LS} can be derived briefly due to constant d_{MELT} by comparing the heat flux thorough molten flux film and steel shell as

$$k_{EFF(MELT)}(T_{LS} - T_{CL})/d_{MELT} = k_{COND(SHELL)}(T_{LS} - T_{CL})/d_{SHELL} \quad \text{.....(A-5)}$$

$$T_{LS} = (R_{MELT}T_S + R_{SHELL}T_{CL})/(R_{MELT} + R_{SHELL}) \quad \text{.....(A-6)}$$

Appendix B. Calculation of Radiative Thermal Conductivity

When the interfacial temperatures and thicknesses of crystalline and molten layers of mold flux film are defined as shown in Fig. 1, radiative thermal conductivity of mold flux film can be calculated on gray gas assumption as

$$q_{RAD} = k_{RAD}(T_{LS} - T_{CL})/d_{MELT} \quad \text{.....(A-7)}$$

$$k_{RAD} = \beta(T_{LS}^4 - T_{CL}^4)d_{MELT}/(T_{LS} - T_{CL}) \quad \text{.....(A-8)}$$

$$\beta = n^2\sigma/(0.75\alpha d_{MELT} + 1/\varepsilon_{STEEL} + 1/\varepsilon_{CRY} - 1) \quad \text{.....(A-9)}$$

In Eq. (A-9), α is average absorption coefficient over the whole wavelength. In this study, an apparent average absorption coefficient, α_P, is chosen as

$$\alpha_P = -\partial[\log Tr(x)]/\partial x \quad \text{.....(A-10)}$$

$$Tr(x) = \int [e_{\lambda b}\exp(-\alpha_\lambda x)]/e_b d\lambda \quad \text{.....(A-11)}$$

$$e_{\lambda b} = 2\pi hc_0^2/\{\lambda^5[\exp(hc_0/k\lambda T) - 1]\} \quad \text{...(A-12)}$$

For crystalline layer, Eqs. (A-7) to (A-9) are rearranged as

$$q_{RAD} = k_{RAD}(T_{CL} - T_{MC})/d_{CRY} \quad \text{.....(A-13)}$$

$$k_{RAD} = \beta(T_{CL}^4 - T_{MC}^4)d_{CRY}/(T_{CL} - T_{MC}) \quad \text{.....(A-14)}$$

$$\beta = n^2\sigma/(0.75\alpha d_{CRY} + 1/\varepsilon_{MOLD} + 1/\varepsilon_{STEEL} - 1) \quad \text{....(A-15)}$$

Total heat flux near the meniscus in mold can be calculated by introducing effective thermal conductivity, k_{EFF}, on an assumption that there are no interaction between conduction and radiation:

$$q_{TOT} = k_{EFF(MELT)}(T_{LS} - T_{CL})/d_{MELT} \quad \text{.....(A-16)}$$

$$q_{TOT} = k_{EFF(CRY)}(T_{CL} - T_{MC})/d_{CRY} \quad \text{.....(A-17)}$$